Proceedings World Geothermal Congress 2000
Kyushu - Tohoku, Japan, May 28 - June 10, 2000

A NEW GEOCHEMICAL MODEL OF THE YANGBAJING GEOTHERMAL FIELD, TIBET

Zhao Ping[1], Dor Ji[2] and Jin Jian[1]
[1]Institute of Geology and Geophysics, Chinese Academy of Sciences, P.O.Box 9825, Beijing, 100029, P.R.China
[2]Geothermal Geological Team of Tibet, No. 15 Jingzhuxilu, Lhasa, 850000, P.R.China

Key Words: geothermal, geochemistry, isotope, geochemical model, Yangbajing Geothermal Field, Tibet

ABSTRACT

Drilling and geochemistry data show the Yangbajing Geothermal Field consists of two reservoirs, a shallow one at depths less than 450 m with temperature of 150~165°C, and a deep one at depths of 950 to 1336m with temperatures as high as 251°C. Waters from both reservoirs are sodium chloride and have the same B/Cl ratio, implying a common origin. Quartz and chalcedony geothermometers are applicable to the deep and shallow reservoirs respectively. Hydrogen and oxygen isotopes suggest both thermal waters are of meteoric origin. The recharge area is the south slope of the Nyainquentanglha Range located northwest of the field.

Carbon dioxide is the main non-condensable gas component in the field. Helium isotopic ratios and a He-Ar-N_2 diagram indicate a predominately crustal origin of the gases. Carbon dioxide is inferred to be derived from partial melting of the Nyainqentanglha core complex.

A new geochemical model shows heat and gases from molten crust in the Nyainquentanglha core complex at a depth of 5 km rising up to a 250°C deep reservoir in fractured Himalayan granite. Thermal fluid rises from this deep reservoir to a cooler and shallower reservoir primarily in Quaternary alluvium. The thermal fluid is modified by degassing, oxidation, mixing, and precipitation processes prior to reaching the surface.

1. INTRODUCTION

The Yangbajing Geothermal Field is located 94 km northwest of Lhasa, the capital of the Tibet Autonomous Region, at elevations ranging from 4290 to 4450 m above sea level (Fig. 1). The total installed capacity at the field is 25.18 MW_e. It supplies half of the electrical load of Lhasa's grid. Since the first geothermal well was completed in 1976, more than 80 wells have been drilled in the region. A shallow reservoir was found at depths less than 450 m, with temperatures varying between 150°C and 165°C and decreasing toward the southeast. Recently, the pressure in the production wells has sharply declined. Now there is insufficient steam available to run the turbines at full load (Zhao et al., 1997). To explore for new geothermal resources, two deep wells, ZK4002 and ZK4001, were drilled in the northern field (Fig. 1). Well ZK4002 was completed at 2006.8 m in December 1993. At the beginning of a 1994 flow test, the wellhead temperature and pressure were 200°C and 1.5 MPa respectively. Unfortunately, both values decreased with time, stabilizing at 125°C and 0.14 MPa. The well produced 2100 kJ/kg fluids but discharge was intermittent. A May 1994 temperature log measured 329°C at 1850 m. The well will not be used for power generation due to its low permeability. Well ZK4001, 370 m southeast of well ZK4002, was targeted to a depth of 2000 m, but drilling was stopped at 1450 m in November 1996. A shallow production zone of 170°C in this well is in fractured Himalayan granite between 240 and 450 m. A deeper production zone with an average temperature of 248°C is at depths of 950 to 1336 m. During production tests, the flowrate stabilized after only 20 minutes at wellhead conditions of 200°C and 1.5 MPa with two-phase fluid flowing at 84 kg/s.

2. GEOLOGY

The Yangbajing Geothermal Field is situated in a Cenozoic basin that stretches towards the southwest (Dor Ji and Zhao Ping, 2000). The basin is bordered by the Nyainquentanglha Mts. on the northwest and the Tang Mts. on the south. Basement rocks are the Nyainquentanglha group that consists of paragneisses intercalated with granitic gneiss and amphibolite. There are two primary fault orientations in the field, NE-SW and NW-SE striking. The latter dominates geothermal water migration in the field. The China-Nepal highway divides the field into two parts, the southern and northern. The topographically lower southern part is covered by Quaternary alluvium underlain by Himalayan granite and tuff. The thickness of the alluvium ranges from 100 to 300 m. Opal and calcite precipitate from the thermal water to form a self-sealed alluvium cap. Altered granite with a small amount of volcanic breccia underlies the northern part. The granite is often replaced by kaolinite and drilling cores of well ZK4002 give a K-Ar age of 7.6 Ma. The volcanic breccia has a K-Ar age 46 Ma, much older than the granite. The granite is fractured at depth in the northern part of the field. Pervasive sericite and chlorite alternation is present in mylonite gneiss with biotite also being chloritized. Stratigraphic columns of wells ZK308, ZK354, ZK355, ZK4001 and ZK4002 are shown in Figure 2. A magnetotelluric survey, performed by UN/DDSMS in 1995, revealed a resistivity anomaly at a depth of 5 km in the northern part of the field, which is inferred to be a magmatic body (Zhao et al., 1998a).

3. FLUID GEOCHEMISTRY

3.1 Water Chemistry

Four different water types have been recognized in the vicinity of the Yangbajing Geothermal Field: sodium chlorite, sodium bicarbonate, calcium bicarbonate, and bicarbonate- and sulfate-rich waters. The shallow and deep thermal waters are sodium chlorite and have little magnesium (Table 1). Sodium bicarbonate waters outcrop as warm springs and are a mixture of the chloride thermal water and cold groundwater. Due to declining pressures these waters no longer discharge at the surface. Cold groundwaters in Quaternary strata, rivers, and meteoric waters are calcium bicarbonate, with small amounts of nitrate. Bicarbonate-rich and sulfate-rich waters are mostly acidic, and represent cold groundwater heated by CO_2- and H_2S-rich steam. A typical such water is enriched in calcium sulfate and occurs near fumaroles or steaming ground.

Lake Nam Co is located on the north side of the Nyainquentanglha Range, about 60 km north of Yangbajing. It is the biggest saline lake in the Tibetan Plateau and one of three holy lakes in Tibet. Basement rocks beneath Lake Nam Co are Carboniferous carbonates. The lake is at an elevation of 4718 m, and higher than Yangbajing. In the past years, it has been suggested that the lake water, by virtue of a strong hydraulic pressure drive, flowed down to the Yangbajing Field along a deep regional tectonic zone. However, geochemical data show distinct differences in chemical compositions between the Lake Nam Co water and the Yangbajing thermal waters. The Yangbajing thermal waters are sodium chloride and contain very little magnesium but the lake water is sodium bicarbonate and contains much magnesium and sulfate (Table 1). The lake water has δD of -74.8‰ and $\delta^{18}O$ of -7.09‰, and so is enriched in ^{18}O and D relative to the thermal waters (Fig. 5). These results argue against Lake Nam Co being a potential recharge area of the Yangbajing fluid because rock minerals contain little hydrogen, and water rock interaction seldom changes hydrogen isotope ratios (Zhao et al., 1998b).

Since well ZK4001 successfully encountered a deep reservoir in 1996, it has become essential to understand the relationships between the shallow and deep reservoirs prior to installing or modifying turbines. The Na/K ratios of thermal waters collected in the production wells range from 7.7 to 8.9. The Na-K geothermometer gives subsurface temperatures in the range of 207~225°C, which is higher than the measured temperatures in the shallow reservoir (see column $T_{Na\text{-}K}{}^3$ in Table 2). During the drilling of wells ZK4001 and ZK4002, no production was found at these temperatures. The Na/K ratio of well ZK4001 is 5.1 and the Na-K temperature of 275.6°C is also higher than the measured temperature. There is no linear relationship between sodium and potassium concentrations for all hot water samples, but the relationship between chlorite and boron is linear (Fig. 3). This implies the shallow thermal water is a mixture of the deep thermal water and the cold groundwater. The mixing process does not seem to have any impact on the Na/K ratios of the thermal waters because the cold groundwater contains very little sodium and potassium. Water-rock interactions in the shallow fractured granite is believed to change the Na/K ratio toward re-equilibrium. Mineral equilibrium simulation of well ZK355 indicates most of the minerals are close to equilibrium at a temperature of 154°C. In most wells, the chalcedony geothermometer agrees more closely with the measured temperature in the shallow reservoir while the quartz geothermometer is applicable to the deep reservoir. The high measured temperatures in well ZK4002 and the low Na/K ratio of the deep thermal waters suggest the possibility of a deeper production zone, with a temperature exceeding 270°C.

3.2 Non-condensable Gas Chemistry

Carbon dioxide is the dominant non-condensable gas component at Yangbajing, usually higher than 90% by volume. The H_2S content is in the range 0.2~0.5%, H_2 in the range 0.02~0.23%, CH_4 less than 0.2%, He in the range 44~1167 ppm and SO_2 in 10^{-9} range. The data presented in Table 3 have not been corrected for air contamination. Giggenbach (1992) suggested that relative He, Ar and N_2 contents could be used to differentiate gas samples from geothermal and volcanic systems (Fig. 4). N_2/Ar and Ar/He ratios are 84 and 1800 in air respectively. The N_2/Ar ratio of meteoric water is 38 and its Ar/He ratio is about 6800. Andestic gases associated with convergent plate boundaries have N_2/Ar ratios of 2500 to 5000 and N_2/He ratios of 1700 to 5000. Basaltic and crustal gases are characterized by high helium contents and He/Ar ratios. However, they are difficult to distinguish from each other on the He-Ar-N_2 triangular diagram. A reliable way is to determine the $^3He/^4He$ ratios.

Non-condensable gases can be divided into two categories at Yangbajing. One includes the samples collected from wells ZK4001, ZK4002, ZK201 and the Regou fumarole. Gases from these locations are inferred to originate directly from the deep reservoir with high He and CH_4 contents and similar steam compositions, i.e. CO_2 308~368 mmol/kg steam, H_2S 1.62~4.63 mmol/kg, H_2 0.06~0.23 mmol/kg and CH_4 0.21~0.40 mmol/kg. The positions of data points are close to the He corner in Figure 4. The N_2/Ar ratios of these samples are greater than 38 (in meteoric water) and 84 (in air). It indicates the nitrogen has non-atmospheric origin, probably derived from metamorphism.

The other category consists of the samples collected from shallow production wells. In these, the total gas content is low in the steam, normally CO_2 20~50 mmol/kg steam, H_2S 0.1~0.6 mmol/kg and H_2 0.01~0.03 mmol/kg. The positions of these data points are scattered on the triangular diagram. It indicates that cold groundwater carries dissolved atmospheric components into the reservoir. A small amount of methane is present in these samples. There is a little gas in the steam from shallow wells ZK357, ZK358 and ZK359. Their gas/condensate ratios are less than 0.1 l/kg. The thermal waters in these wells are believed to degas in the reservoir prior to approaching the boreholes. These data suggest that the Yangbajing geothermal gases have a crustal origin (Zhao et al., 1998c).

4. ISOTOPE GEOCHEMISTRY

4.1 Hydrogen and Oxygen Isotopes

A regional monsoonal weather pattern results in variable precipitation rates and meteoric isotopic compositions. For example, a sample collected in August 1995 at Yangbajing was rich in D and ^{18}O with –82.3‰ for δD and –11.59‰ for $\delta^{18}O$. A September 1996 sample was depleted in heavy isotopes, -231.5‰ for δD and –30.76‰ for $\delta^{18}O$. It is not easy to construct a local meteoric water line, but the meteoric line of Lhasa is available and is used as the reference. Due to the lack of downhole collection tools, the thermal waters were collected at the wellhead after cooling to prevent steam loss. The stable isotopic composition of the thermal water is -151~-161‰ for δD and -17.73~-19.54‰ for $\delta^{18}O$ (Fig. 5). The deep thermal water is slightly richer in D and ^{18}O than the shallow thermal water. The thermal waters at Yangbajing are of meteoric origin and the oxygen isotope shift is not more than 2.1‰. The thermal water recharge area is believed to be northwest of the field, on the south slope of the Nyainquentanglha Range, at elevations near 4800 m.

4.2 Helium Isotopes

The ^4He isotope is a product of the decay of U and Th. ^3He is generated by the nuclear reaction of $^6Li(n,\alpha)^3H(\beta)^3He$.

Helium isotopic compositions depend on concentrations of U, Th and Li in rocks (Mamyrin et al., 1984). The $^3He/^4He$ ratio of air (Ra) is 1.4×10^{-6}. The average R/Ra ratio of crustal radiogenic helium is expected to be 0.02 while the R/Ra ratio is as high as 8.1 for middle oceanic ridge basalt (Lupton, 1983). Helium in the thermal fluids may come from atmosphere, crustal or mantle sources. Atmospheric helium is dissolved in meteoric water and transported into reservoirs. The R/Ra ratio of the deep Yangbajing fluid is slightly higher than in the shallow one, with both ratios being less than 0.5. It implies the helium is mainly generated by the crust and mixed with a small atmospheric component. Recent cooperative research with the Lawrence Berkeley National Laboratory has built a helium isotope model to explain the mixing of the deep and shallow gases.

4.3 Carbon Isotopes

Among the samples collected from the Regou fumarole and wells ZK201 and ZK4001, lower flowrates correlate with higher CO_2 contents and the higher $\delta^{13}C$ values. The enthalpy of the ZK4001 geothermal fluid is about 1090 kJ/kg. If fluid migration is an adiabatic process in the borehole, it is calculated that the steam fraction can be as high as 0.30 at 100°C and 97% of the CO_2 would enter the vapor phase. Thermodynamic simulation confirms there is no calcite scaling on the ZK4001 wellbore. Therefore, the measured $\delta^{13}C$-CO_2 value actually represents the original deep reservoir composition. There is carbon dioxide and steam removal at the Ragou fumarole and in well ZK201 during the fluid's ascent. This concentrates the carbon dioxide and the residual become isotopically heavier.

No distinctive difference is observed in the $\delta^{13}C$-CO_2 values between the shallow and deep reservoirs. The CO_2 in both reservoirs have the same origin. Wells ZK354, ZK355 and ZK359 are close to the upflowing area in the field. The $\delta^{13}C$-CO_2 values in these wells are similar to that of well ZK4001. The CO_2 slightly enriches ^{13}C in the production wells. Nearly 80% of the CO_2 would be in the state of over-saturation after mixing of the deep thermal water and cold groundwater. Part of the CO_2 will leave from the fluids, such as CO_2-rich vapor escaping or forming calcite. The latter could be observed on the cores of wells ZK4001 and ZK4002. The removal of the CO_2 will affect the $\delta^{13}C$-CO_2 value. The CO_2 in the Yangbajing Geothermal Field is neither mantle-derived nor of marine carbonates origin; it is inferred to originate from metamorphic processes of the Nyainqentanglha core complex. The dynamic source is partial melting of the crust in the depths.

4.4 Sulphur Isotopes

Sulphur isotopic compositions change with valence in geothermal fluids. There are some differences in the $\delta^{34}S$-H_2S and $\delta^{34}S$-SO_4 values between the deep and shallow fluids. Measured H_2S and SO_4^{2-} concentrations are 0.9mmol/kg and 0.2mmol/kg respectively in the total deep discharge and 0.06mmol/kg and about 0.34mmol/kg respectively in the total shallow discharge. The H_2S concentration is controlled by mineral buffers and is an exponential function of reservoir temperatures (Zhao et al., 1996). The deep fluid mixing with the cold groundwater leads the H_2S species to over-saturate in the shallow reservoir and deposit pyrite and other sulphur-bearing minerals. The H_2S may also escape from the shallow reservoir. Part of the H_2S would be oxidized into SO_4^{2-} species during the fluid's ascent. These processes induce a variable isotopic composition in the residual H_2S. The isotopic equilibrium between H_2S and SO_4^{2-} species is very difficult to approach under the conditions of the shallow and deep reservoirs at Yangbajing.

5. CONCLUSIONS

The Yangbajing Geothermal Field is the first geothermal field exploited for power generation in Tibet. The genesis of the geothermal system had been debated for a long time prior to the drilling of wells ZK4002 and ZK4001. Geophysical surveys and recent exploration suggest it is a typical hydrothermal convective system and the heat source is partial melting of the crust at depth, caused by the convergent collision between the Indian and Eurasian plates. Two reservoirs in the Yangbajing Geothermal Field have been found at different depths. The shallow reservoir temperature is in the range 150~165°C. The deep reservoir temperature is about 248°C. Both thermal waters are sodium chlorite and have the same B/Cl ratio which indicates they have a common origin and the shallow thermal water is a mixture of the deep reservoir and cold groundwater (Fig. 6). It is possible to discover a deep, high-flowrate feed-zone, in which the temperature is expected to exceed 270°C.

Helium isotopic composition and the He-Ar-N_2 diagram show the gases originating from the crustal materials. Carbon dioxide is thought to originate from metamorphic processes in the Nyainqentanglha core complex. Stable isotope data indicates the thermal waters in both reservoirs are of local meteoric origin. The oxygen isotope shift is observed in the isotope compositions of the thermal waters. The quantity and isotopic composition of H_2S and SO_4^{2-} species will be variable during the fluid's ascent. It is expected that exploitation of the deep reservoir will accelerate depletion of the shallow reservoir but it will increase the power generation capacity because the deep thermal water has higher enthalpy and generation efficiency.

ACKNOWLEDGEMENTS

The authors are very grateful to two anonymous reviewers for their reviewing and editing. The research project is funded by the National Natural Science Foundation of China (Grant No. 49672168) and International Atomic Energy Agency (Grant No. 9095).

REFERENCES

Arnorsson, S. (1985). The use of mixing models and chemical geothermometers for estimating underground temperatures in geothermal systems. *J. Volcanic Geothermal Res.*, Vol.23, pp. 299-335.

Arnorsson, S., Gunnlaugsson, E. and Svavarsson, H. (1983). The chemistry of geothermal waters in Iceland, III. Chemical geothermometry in geothermal investigations. *Geochim. Cosmochim. Acta*, Vol.47(3), pp. 567-577.

Dor Ji and Zhao Ping. (2000). Characteristics and genesis of the Yangbajing Geothermal Field, Tibet. In: *Proceedings of the World Geothermal Congress, 2000*.

Fournier, R.O. (1977). Chemical geothermometers and mixing models for geothermal systems. *Geothermics*, Vol.5(1), pp. 41-50.

Fournier, R.O. (1979). A revised equation for the Na/K geothermometer. *Geothermal Resources Council Transactions*, Vol.3, pp. 221-224.

Giggenbach, W.F. (1992). The composition of gases in geothermal and volcanic systems as a function of tectonic setting. In: *Proceedings of the 7th International Symposium on Water-Rock Interaction*, Y.K. Kharaka and A.S. Maest (Eds)., A.A.Balkema, Rotterdam, pp. 873-878.

Lupton, J.E. (1983). Terrestrial inert gases: isotope tracer studies and clues to primordial components in the mantle. *Annual Review of Earth and Planetary Science*. Vol.11, pp. 317-414.

Mamyrin, B.A. and Tolstikhin, I.N. (1984). *Helium Isotope in Nature*. Elsevier, Amsterdam, 273 pp.

Zhao Ping and Armannsson, H. (1996). Evaluation and interpretation of gas geothermometry results for selected Icelandic geothermal fields with comparative examples from Kenya. *Geothermics*, Vol.25(3), pp. 307-347.

Zhao Ping, Dor Ji and Liang Tingli. (1997). Deep geothermal resources in the Yangbajing field, Tibet. *Geothermal Resources Council Transactions*, Vol.21, pp. 227-230.

Zhao Ping, Jin Jian, Zhang Haizheng, Dor Ji and Liang Tingli. (1998a). Gas geochemistry in the Yangbajing geothermal field, Tibet. In: *Proceedings of the 9th International Symposium on Water-Rock Interaction*, G.B. Arehart and J. Hulston (Eds)., A.A.Balkema, Rotterdam, pp. 657-660.

Zhao Ping, Jin Jian, Zhang Haizheng, Dor Ji and Liang Tingli. (1998b). Chemical Composition of thermal water in the Yangbajing geothermal field, Tibet (in Chinese, with English abstract). *Scientia Geologica Sinica*, Vol.33(1), pp. 61-72.

Zhao Ping, Dor Ji, Liang Tingli, Jin Jian and Zhang Haizheng. (1998c). Characteristics of gas geochemistry in the Yangbajing geothermal field, Tibet. *Chinese Science Bulletin*, Vol.43(21), pp. 1770-1777.

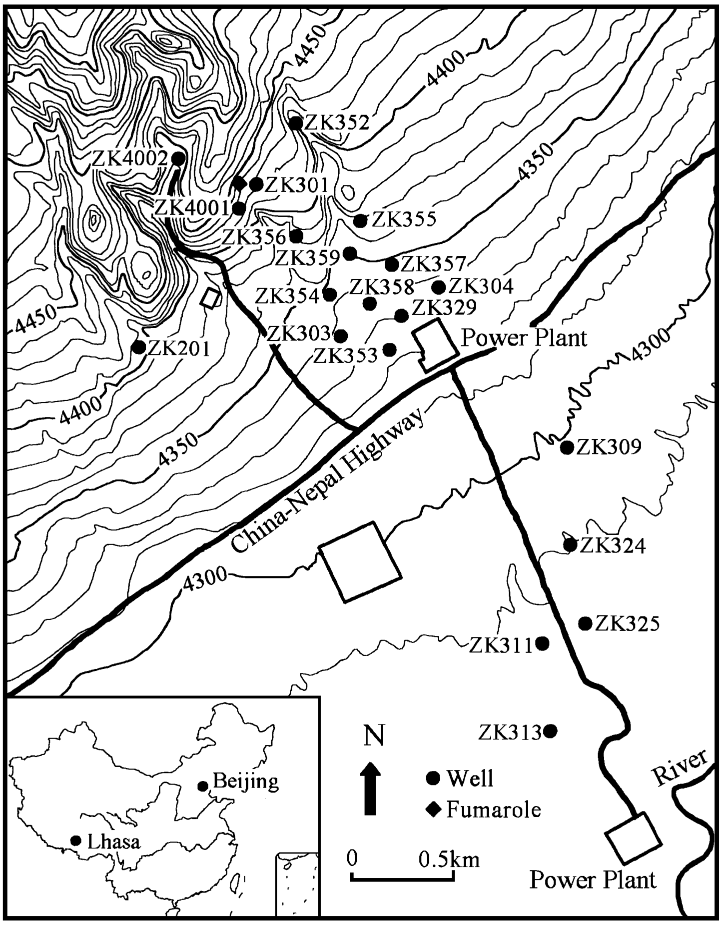

Figure 1. Location Map of the Yangbajing Geothermal Field, Tibet

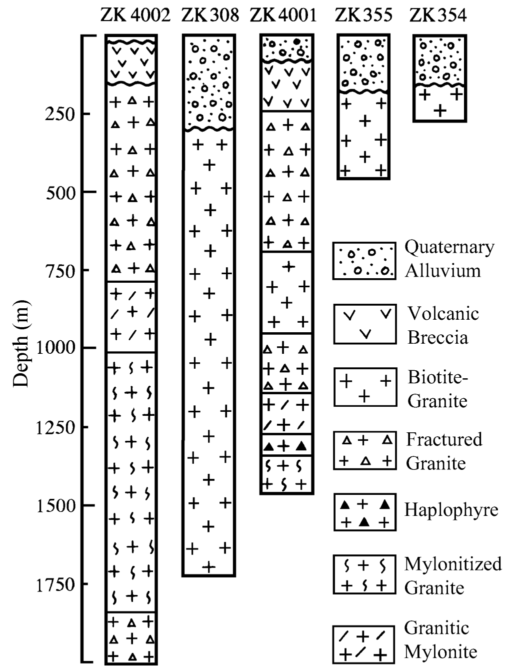

Figure 2. Stratigraphic Columns of Wells ZK308, ZK354, ZK355, ZK4001 and ZK4002

Table 1. Chemical compositions of the thermal and cold waters in the Yangbajing geothermal field, Tibet (in ppm)

Location	Date	pH	SiO_2	CO_2	H_2S	Li	Na	K	Ca	Mg	B	Al	Fe	F	Cl	SO_4	NO_3
ZK311	95.09.16	5.69	67	n.a.	n.a.	2.4	99	12.8	0.91	<0.05	11.2	<0.01	<0.01	3.3	112	8.9	n.d.
ZK313	95.09.12	8.86	205	214.7	0.34	10.3	417	48.4	1.89	0.10	42.0	<0.01	<0.01	13.2	479	32.8	n.d.
ZK325	95.08.18	8.82	206	120.8	0.63	7.5	328	38.5	3.99	0.10	37.3	0.03	<0.01	13.7	415	35.6	n.d.
ZK309	96.09.21	8.88	224	61.6	0.48	7.6	338	44.2	3.64	<0.01	50.6	0.16	<0.01	14.7	472	40.8	n.d.
ZK329	95.08.26	8.89	214	83.0	0.21	8.1	337	39.6	4.40	0.10	41.7	0.13	0.10	14.9	481	39.7	n.d.
ZK303	95.09.13	8.21	216	125.8	0.42	7.6	316	35.7	3.57	<0.05	36.7	0.03	<0.01	13.2	412	33.8	n.d.
ZK304	95.09.12	8.17	217	126.2	0.70	8.1	332	41.7	3.89	<0.05	39.5	<0.01	<0.01	13.2	451	34.6	n.d
ZK346	95.08.29	8.80	238	83.3	1.02	9.1	377	44.8	3.70	<0.05	45.4	0.05	0.10	14.2	491	38.1	n.d.
ZK354	95.08.21	8.93	248	102.8	0.96	9.4	387	45.8	3.19	0.10	45.6	0.01	0.10	14.3	513	38.4	n.d.
ZK355	95.09.13	8.49	241	119.7	0.89	9.2	408	47.3	3.56	<0.05	44.5	0.16	<0.01	14.6	489	37.7	n.d.
ZK356	95.08.30	8.90	260	121.5	0.63	10.3	421	55.6	2.82	<0.05	47.2	0.03	0.03	14.0	531	39.6	n.d.
ZK357	95.09.15	8.94	247	86.2	0.21	9.1	383	48.4	3.97	<0.05	44.4	0.09	0.03	15.1	519	39.9	n.d.
ZK359	96.09.19	8.92	256	92.3	0.71	8.7	370	47.5	2.84	<0.01	55.7	0.20	<0.01	14.4	514	43.2	n.d.
ZK4001	96.11.13	8.66	684	174.3	0.82	20.9	547	107.3	2.16	<0.01	96.7	2.11	0.02	12.8	891	25.9	n.d.
ZK4002	96.11.10	6.32	350	422.4	0.14	32.4	684	159.7	10.6	0.16	125	0.33	0.31	13.5	1134	56.5	n.d.
Zangbuqu[1]	95.08.20	8.20	9.3	37.7	<0.03	0.03	3.7	0.93	14.9	1.81	0.38	0.49	0.64	0.3	0.7	6.5	0.2
Luziqu[2]	96.09.11	7.95	5.6	22.0	<0.03	<0.01	1.0	0.70	13.4	1.08	0.13	0.25	0.06	0.5	0.1	10.9	1.3
Caoyuan[2]	95.08.20	8.17	8.1	28.3	<0.03	0.01	1.0	0.52	14.6	1.88	0.50	0.12	0.10	0.2	0.2	7.9	0.4
Dianchang[3]	95.09.18	7.40	13.2	37.7	<0.03	0.01	10.0	2.06	25.6	3.39	0.28	<0.01	0.03	0.4	13.8	16.6	21.5
Snow[4]	95.09.20	n.a.	n.a.	n.a.	n.a.	<0.01	3.6	1.14	<0.05	<0.05	0.17	<0.01	<0.01	0.05	4.8	0.3	1.2
Nam Co[5]	96.08.27	9.20	0.34	616	<0.03	0.69	307	36.1	6.7	83.6	3.33	0.03	<0.01	0.97	68.2	204	n.d.

1, river. 2, surficial water. 3, cold water aquifer. 4, collected at an elevation of 5360m above sea level. 5, saline lake.
"n.a.", not analysis. "n.d.", not detect.

Table 2. Calculated results of different geothermometers (°C)

Locations	Tc	Tqtz[1]	Tqtz[2]	TNa-K[3]	TNa-K[4]
ZK313	148.4	171.7	169.5	210.7	230.1
ZK325	148.7	172.0	169.8	211.9	231.1
ZK309	153.9	176.8	174.5	224.1	241.1
ZK329	151.1	174.2	171.9	212.1	231.2
ZK303	151.7	174.7	172.5	207.8	227.7
ZK304	151.9	175.0	172.7	219.5	237.3
ZK346	157.8	180.4	178.0	213.3	232.2
ZK354	160.4	182.9	180.4	212.8	231.9
ZK355	158.6	181.1	178.8	210.6	230.0
ZK356	163.5	185.7	183.2	225.2	242.1
ZK357	160.1	182.6	180.2	220.2	237.9
ZK359	162.5	184.8	182.3	221.9	239.4
ZK4001	237.6	253.6	249.0	275.6	282.5

Tc, chalcedony geothermometer, maximum steam loss (Arnorsson et al., 1983).
Tqtz[1], quartz geothermometer, maximum steam loss (Arnorsson, 1985).
Tqtz[2], quartz geothermometer, maximum steam loss (Fournier, 1977).
TNa-K[3], Na-K geothermoeter (Arnorsson et al., 1983).
TNa-K[4], Na-K geothermometer (Fournier, 1979).

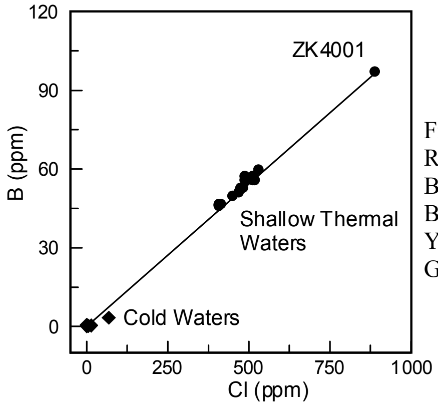

Figure 3. Relationship Between Cl and B Contents in the Yangbajing Geothermal Field

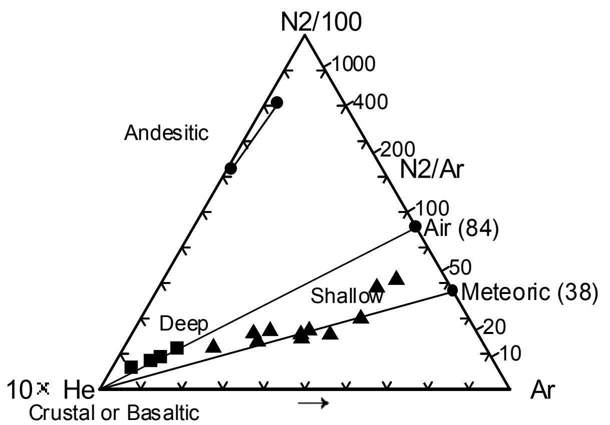

Figure 4. He-Ar-N_2 Diagram (modified from Zhao et al., 1998c)

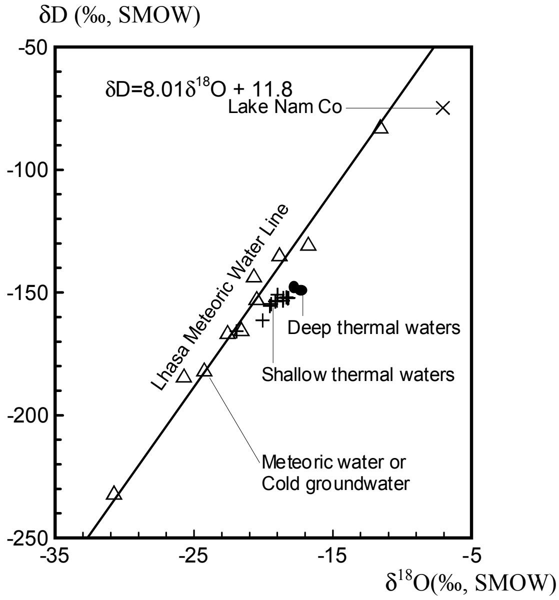

Figure 5. Relationship of δD vs. $\delta^{18}O$

Table 3. Chemical and carbon isotopic compositions of non-condensable gases in the Yangbajing geothermal field, Tibet (modified from Zhao et al., 1998c)

Location	Depth (m)	CO_2 (%)	H_2S (%)	H_2 (%)	CH_4 (%)	N_2 (%)	He (%)	Ar (%)	O_2 (%)	$\delta^{13}C$-CO_2 (‰, CDT)
ZK311	82	95.2	0.40	0.025	--	4.06	0.0095	0.10	1.06	
ZK313	155	94.5	0.23	0.018	0.02	4.14	0.0121	0.08	1.40	-9.88
ZK325	95	92.5	0.22	0.035	--	6.17	0.0078	0.16	0.59	-8.61
ZK324	130	94.7	0.38	0.041	0.03	3.54	0.0094	0.09	1.06	-10.03
ZK309	140	85.7	0.27	0.028	--	11.7	0.0044	0.21	2.28	-10.83
ZK304	207	93.8	0.33	0.041	--	4.67	0.0104	0.14	0.47	-8.76
ZK329	240	92.5	0.34	0.074	0.03	6.15	0.0204	0.11	1.20	-7.72
ZK355	454	95.0	0.42	0.036	0.03	3.14	0.0121	0.07	1.20	-10.29
ZK359	270	77.2	0.35	0.028	--	17.2	0.0104	0.31	4.21	-10.16
ZK303	336	92.7	0.23	0.034	--	5.02	0.0145	0.14	0.92	
ZK354	273	93.2	0.43	0.064	0.03	4.03	0.0215	0.07	1.55	-11.33
ZK201	270	90.4	0.33	0.227	0.10	8.03	0.0519	0.09	1.40	-8.94
ZK4002	2006	89.2	0.52	0.036	0.15	8.12	0.1167	0.06	1.38	
ZK4001	1495	91.3	0.40	0.017	0.08	5.86	0.0601	0.06	0.74	-11.01
Regou*		94.5	0.18	0.058	0.10	5.38	0.0472	0.06	0.56	-7.84

"*", fumarole.

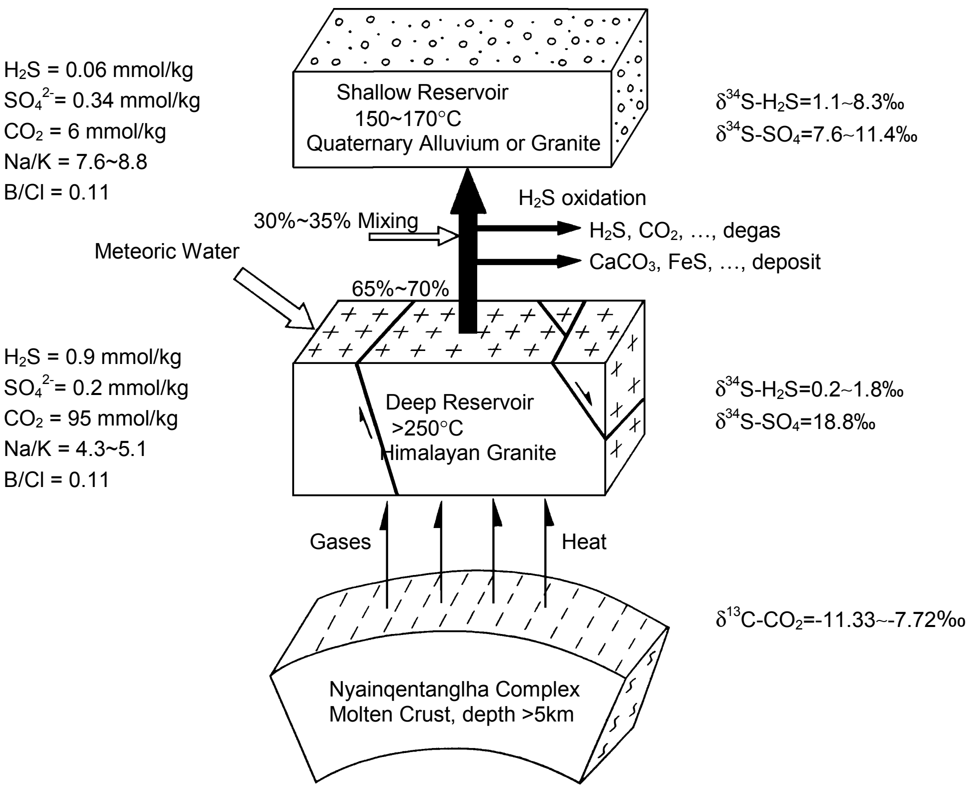

Figure 6. Conceptual Geochemistry Model of the Yangbajing Geothermal Field, Tibet